

Optical Engineering

SPIEDigitalLibrary.org/oe

Mode-locked 2- μ m wavelength fiber laser using a graphene-saturable absorber

Marc Currie
Travis Anderson
Virginia Wheeler
Luke O. Nyakiti
Nelson Y. Garces
Rachael L. Myers-Ward
Charles R. Eddy, Jr.
Fritz J. Kub
D. Kurt Gaskill



Mode-locked 2- μm wavelength fiber laser using a graphene-saturable absorber

Marc Currie
 Travis Anderson
 Virginia Wheeler
 Luke O. Nyakiti
 Nelson Y. Garces
 Rachael L. Myers-Ward
 Charles R. Eddy, Jr.
 Fritz J. Kub
 D. Kurt Gaskill
 U.S. Naval Research Laboratory
 Optical Sciences and Electronics Science and
 Technology Divisions
 Washington, DC 20375
 E-mail: marc.currie@nrl.navy.mil

Abstract. Soliton-like pulses with a 1984-nm center wavelength are produced from a Tm-doped mode-locked fiber laser. The linear cavity has a graphene saturable absorber mirror at one end and a fiber Bragg grating as the output coupler. The laser operates without dispersion compensation, and the repetition rate was tuned from 20 to 5 MHz by the addition of SMF-28 fiber. The dry transfer process used to place the graphene on a mirror could be extended to any optical substrate. This enables integration of graphene with optics such as an optical window coated with a graphene filter or a graphene-saturable absorber placed directly on a semiconductor laser facet. © The Authors. Published by SPIE under a Creative Commons Attribution 3.0 Unported License. Distribution or reproduction of this work in whole or in part requires full attribution of the original publication, including its DOI. [DOI: [10.1117/1.OE.52.7.076101](https://doi.org/10.1117/1.OE.52.7.076101)]

Subject terms: lasers; fiber lasers; nonlinear optics.

Paper 130424 received Mar. 15, 2013; revised manuscript received May 28, 2013; accepted for publication Jun. 3, 2013; published online Jul. 1, 2013.

1 Introduction

Graphene is an interesting optical material. It possesses a nearly wavelength independent linear absorption from the visible through the far infrared, while absorbing a large amount (2.3%) of light per monolayer.¹ With a finite number of carriers in the monolayer, Pauli blocking enables graphene to exhibit optical-saturable absorption at low saturation intensities. This effect was first demonstrated and used as a mode-locking element for a fiber laser.²

Since then, mode-locked lasers have been created using graphene as a saturable absorber at wavelengths in the near IR.^{3–10} Theory predicts graphene's performance as a saturable absorber at wavelengths beyond 1.55 μm .⁹ Graphene's broadband performance has been shown by a few groups by using it as a saturable absorber to mode-lock lasers at wavelengths longer than 1.55 μm .^{3,10–12} This is useful since relatively few semiconductor-saturable absorbers (SESAMs) have been created in the mid-infrared region (e.g., wavelengths beyond 2.2 μm). The semiconductor-saturable absorber materials used in this region are GaAs,¹¹ InGaAs,¹³ GaInSb/GaSb,¹⁴ and InAs/GaSb.^{15–17} In addition, graphene's optical damage threshold is high enough (near 100 GW/cm²)¹⁸ to allow saturable absorption without the concern of damaging the graphene.

While graphene-based fiber lasers have been mode locked at 1 and 1.5 μm ,^{3–7} there are only a few reports of graphene as a saturable absorber at 2 μm , such as: two Q-switched lasers,^{11,19} a Q-switched and mode-locked laser,³ a mode-locked solid-state laser,¹⁰ and one (recent) report of graphene's use in mode-locked fiber lasers at a wavelength greater than 1.6 μm .¹²

Of the reported graphene-saturable absorbers, few are fabricated as saturable absorber mirrors (SAMs). Graphene-based SAMs have been fabricated via (1) dispersion of graphene in a solution with poly(methyl methacrylate)²⁰ and polyvinyl-alcohol,²¹ (2) liquid-phase exfoliation of small area ($\sim 20 \mu\text{m}$) flakes,^{8,22,23} or (3) chemical vapor deposition on copper foils and transferral to a mirror.^{3,10}

Until now, epitaxially grown graphene on silicon carbide (SiC) was used as a saturable absorber only in Q-switched lasers,^{9,19,24,25} and not in mode-locked lasers. Here, we report a graphene SAM fabricated using large-area epitaxially grown graphene on SiC and transferred by a unique dry transfer process to an Ag mirror. Our transfer process overcomes an obstacle of growing high-quality large-area graphene and transferring it to substrates suitable for optical devices with area of $1 \times 1 \text{ cm}^2$. This is a tremendous advantage for creating continuous graphene layers over large areas that are unachievable with the popular method of sonication of graphite.^{8,22,23} In addition, using graphene synthesized on SiC opens up a potential avenue for mass production of saturable absorber feedstock. Such an approach will benefit from the obvious economies of scale associated with the commercial business of GaN on SiC LEDs as well as the increasingly important low voltage (600 V) SiC current switches that are of interest for applications such as in the auto industry.

Using this graphene-based SAM, we demonstrate a mode-locked Tm-doped fiber laser in a linear cavity, eliminating additional optical elements used in the more common ring-cavity fiber lasers. Our laser produces soliton-like pulses, whose repetition rate is varied by increasing the cavity length with additional SMF-28 fiber. This laser system provides a path for compact portable sources for spectroscopy in the molecular fingerprint region,²⁶ lab-on-a-chip sensors, and other applications currently served by large laboratory lasers.

2 Experiment

Practical graphene optical devices often require large, uniform, high-quality films measuring at least $5 \times 5 \text{ mm}^2$ and deposited on optically compatible substrates. The most promising synthesis methods for this are graphene epitaxially produced by sublimation of Si from SiC substrates.²⁷ Graphene layers were epitaxially grown on the carbon face of semi-insulating on-axis 6H-SiC substrates. The process was performed at 1600°C under high vacuum

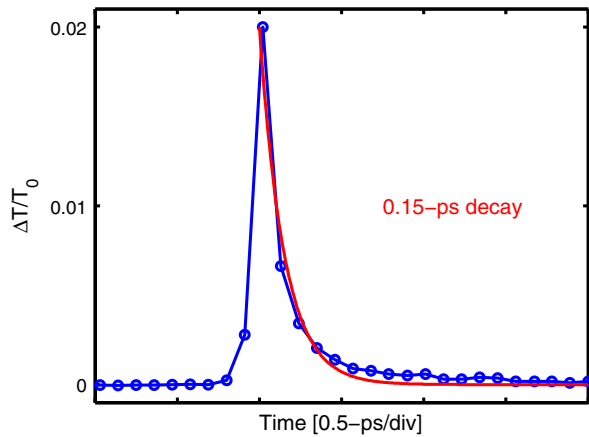


Fig. 1 Multilayer graphene response to 100-fs optical pump-probe measurement demonstrates saturable absorption with a 2% increase in transmission.

($<10^{-4}$ mbar).²⁸ A transmissive scanning optical probe characterized the epitaxially grown graphene as a multilayer structure containing 13 ± 3 layers.

The saturable absorption for multilayer epitaxially grown graphene sample on SiC was measured using degenerate femtosecond optical pump-probe spectroscopy at 800 nm. The results, shown in Fig. 1, demonstrate that in response to a 100-fs optical pulse the multilayer graphene sample undergoes a 2% increase in transmission (Fig. 1). Different graphene-saturable absorber growth methods have demonstrated variability in performance. Recently, the modulation depth of graphene-saturable absorption was modified by doping.²⁹ Our graphene sample's recovery to the steady-state transmission is described by a 0.15-ps exponential decay. The pump pulse's energy was 25 pJ and produced a 9 MW/cm^2 optical irradiance on the graphene sample. Our results agree with other measured saturation intensities of 0.6 to 0.7 MW/cm^2 for multilayer graphene-saturable absorbers.²

The graphene was transferred onto a commercial Ag optical mirror via a dry transfer process.³⁰ This removes the epitaxial graphene from the C-face of 6H-SiC and places it onto the mirror using thermal release tape. The transfer of our multilayer film resulted in graphene thicknesses ranging from 0 to 13 layers of graphene across the 25-mm diameter Ag mirror due to adhesion difficulty with the commercial Ag mirror. Surprisingly, this provided an advantage since the graphene SAM has spatially variable saturable absorption characteristics that can be tuned by laterally moving the mirror (as explained later).

A linear fiber laser was constructed using a wavelength-division multiplexer (WDM, Lightel 793/1980) to couple the pump light into a 0.7-m Tm-doped fiber (Nufern SM-TSF-9/125), as shown in Fig. 2. A fiber Bragg grating (FBG) with 80% reflection at 1984 nm and >2 -nm bandwidth was spliced to the WDM and operated as an output coupler. Following the Tm-fiber, several lengths of SMF-28 single-mode fiber were used to vary the cavity length, and these were butt coupled to the graphene SAM. A five-axis stage controlled the graphene SAM's coupling to the laser cavity and enabled laterally moving the SAM to expose different areas, thereby changing the SAM characteristics.

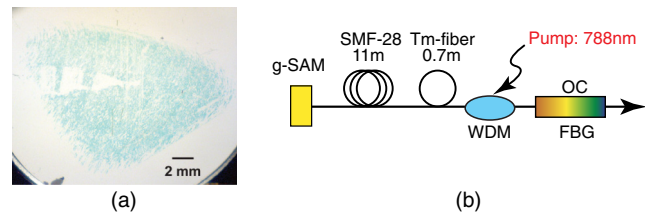


Fig. 2 (a) An image of the graphene transferred to the Ag mirror creating the saturable absorber mirror (SAM). (b) A schematic diagram of the linear fiber laser cavity shows the graphene-based SAM (g-SAM), an optional length of SMF-28 fiber, 0.7-m Tm-doped fiber amplifier, wavelength-division multiplexer (WDM), pump laser, and fiber Bragg grating (FBG) output coupler.

Without the SAM, a 796-nm pump laser was used to obtain the amplified spontaneous emission (ASE) spectrum following the 80% FBG output coupler. Figure 3(a) shows the broad 200-nm-wide ASE spectrum centered at 1820 nm with a 3-nm-wide dip in the curve at 1984 nm due to the FBG reflection, as measured by a Yokogawa AQ 6375 optical spectrum analyzer. The ASE peak <1900 nm is indicative of core-pumped Tm-doped fiber, whereas a cladding-pumped amplifier would have a red-shifted ASE peak near 1950 nm.³¹ (Note: Some residual transmitted 796-nm pump is observed near 1600 nm due to second-order diffraction in the spectrometer, and the apparent spectral noise from 1800 to 1900 nm is due to atmospheric absorption lines within the spectrometer).

The graphene SAM was installed by butt coupling with a SMF-28 fiber. Continuous wave (cw) lasing was achieved at 1984 nm when the SAM was positioned with only the Ag mirror (i.e., in a position with no graphene on the mirror). The losses in the cavity due to the WDM (50% insertion loss at 1984 nm), the output coupler, and the coupling loss at the SAM made it difficult to achieve even cw lasing. Following this, the absorption spectra of the Tm fiber was measured with a white-light source and established 788 nm as the optimal absorption for the Tm fiber. The 796-nm pump was then replaced by a 788-nm fiber-coupled cw Ti:sapphire laser with up to 350 mW coupled into the cavity. This provided >10 -mW cw output from the fiber laser at 1984 nm, which is >150 nm from the Tm fiber's ASE peak.

Lateral motion of the graphene SAM shifted the coupling from the Ag mirror to the graphene coating. In positions with the maximum number of graphene layers, no lasing occurred. In positions with no graphene, cw lasing occurred. In the transition region between no graphene and a few layers of graphene, mode-locked operation occurred. Spectra of the mode-locked operation, shown in Fig. 3(b), demonstrate the mode-locked fiber laser's 1.7-nm spectral width. The spectral wings exhibit Kelly sidebands³² seen in soliton-like saturable absorber lasers that are caused by cavity-enhanced dispersive waves arising from discrete gain, loss, and dispersion in the laser cavity.³³ The broad ASE background is also visible, but is five orders of magnitude weaker than the peak mode-locked signal and can be further minimized by using a bandpass filter (much like the FBG in our laser cavity).

Different lengths of SMF-28 were used to achieve variable repetition rates. Pulsed output was measured with a >100 -MHz bandwidth IR detector (Vigo System

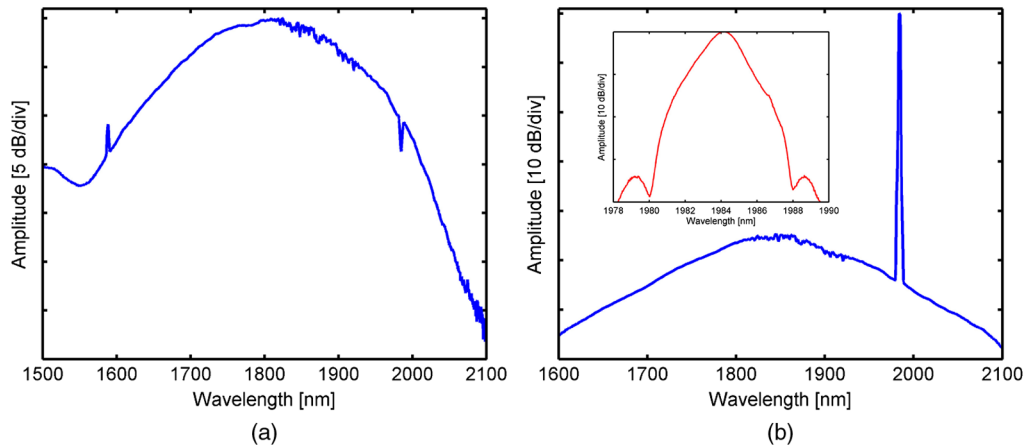


Fig. 3 Optical spectra of the amplified spontaneous emission (ASE) of the Tm fiber (a) and mode-locked laser (b) with inset zooming in on the laser's peak wavelength.

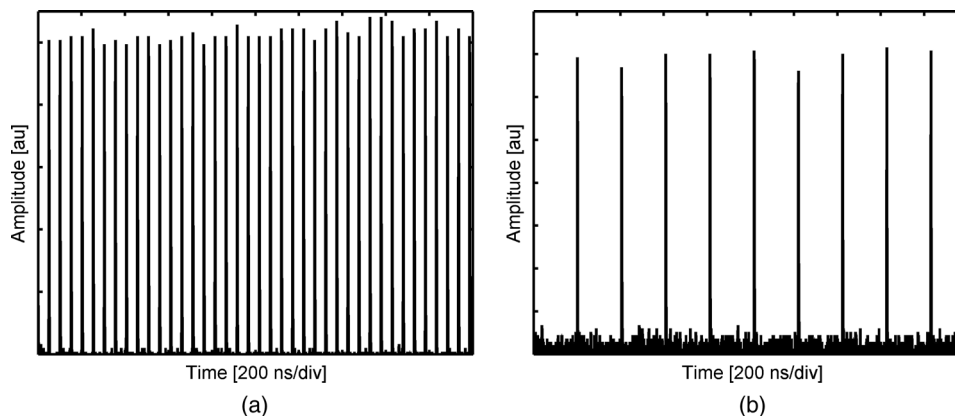


Fig. 4 The temporal response of the detected optical pulse trains shows variable repetition rates of the 19.6-MHz cavity (a) and 4.9-MHz extended cavity (b) using 11-m SMF-28 fiber.

PVM-10.6). Without any additional fiber, the laser had a 19.6-MHz repetition rate, shown in Fig. 4, with a mean temporal spacing of 51 ns and a standard deviation of 0.11 ns, demonstrating a stability better than 0.21% (as measured by a LeCroy WaveRunner oscilloscope). Increasing the cavity length by adding an additional 11 m of SMF-28 fiber produced mode-locked pulses at a 4.9-MHz repetition rate with a stability better than 0.06%. This stability improvement at longer cavity lengths may be caused by slightly higher energy pulses at the saturable absorber, which is offset by the increased attenuation of the additional fiber. At wavelengths near 2 μm , the loss of SMF-28 fiber is large even when wound with diameters >30 cm. For lengths >11 m, the SMF-28 produced intracavity losses that exceeded the system gain, and thus, quenched the laser operation (even cw operation).

With the laser mode-locked, increasing the pump power did not increase pulse's amplitude. Instead, increasing the pump power introduced additional pulses within the cavity repetition rate, at which point the output power would increase in steps of approximately 0.5 mW. Increasing the pump power further increased the number of pulses per cavity round trip with commensurate steps in the output power. With only two or three pulses per cavity round-trip period, the pulses were stable in time (i.e., their temporal spacing

remained fixed). With more than three pulses per round-trip period, the extra pulses were erratic in time, drifting within the laser cavity's round-trip period. Other graphene-based Er-doped fiber lasers near 1550 nm have also demonstrated multiple-soliton dynamics.⁵ During multipulse operation, all of the laser pulses had the same amplitude, which was the same pulse amplitude observed when in single-pulse operation.

3 Results and Discussion

Graphene's saturable absorption characteristics are theoretically predicted to occur over a broad wavelength range.⁹ Our epitaxially grown graphene demonstrated saturable absorption at 800 and 1984 nm. At 800 nm, our pump-probe setup showed a 2% increase in transmission for a 9 MW/cm² optical irradiance. At 1984 nm, the graphene showed mode-locking performance in our laser. To calculate the optical irradiance on the graphene at 1984 nm, we assume that our intracavity power at the output coupler ($P_{\text{out}}/20\% \sim 10 \text{ mW}_{\text{ave}}$) is the same as was present at the graphene-saturable absorber, thereby producing an irradiance on the graphene of 800 MW/cm². This is much greater than the saturation intensity of the graphene² and, combined with the mode-locking of our laser, confirms operation of our graphene-saturable absorber at 1984 nm.

Our laser does not contain any dispersion compensation and, therefore, operates in the anomalous dispersion regime. Pulse evolution in mode-locked lasers occurs through interplay between anomalous group-velocity dispersion (GVD) and nonlinearity (Kerr) within the fiber. When constructed entirely from anomalous-dispersion fiber, this laser can support solitons. With the 11-m SMF-28 extension, the laser cavity is approximately 20 m long (single pass). The GVD of SMF-28 at a 2- μm wavelength is $-0.12 \text{ ps}^2/\text{m}$,³⁴ which provides a rather large round-trip cavity dispersion of 4 ps^2 .

To investigate the soliton-like properties of this laser, we use the ratio of the dispersion to the nonlinear lengths (L_D/L_{NL}) to define the soliton order.³⁵ For a fundamental soliton, the dispersion and nonlinear lengths are equal where the dispersion length ($L_D = T_0^2/|\beta_2|$) and nonlinear lengths [$L_{NL} = 1/(\gamma P_0)$] can be calculated if we know the fiber's GVD (β_2), the pulse width (T_0), the nonlinear parameter (γ), and the peak-pulse power (P_0).

The nonlinear parameter can be calculated as $\gamma = 2\pi n_2/(A_{\text{eff}}\lambda)$, where we use $\lambda = 2 \mu\text{m}$, $n_2 = 2.2 \times 10^{-20} \text{ m}^2/\text{W}$,³⁵ and assume a 15% larger effective area for SMF-28 at 2 μm $A_{\text{eff}} = 100 \mu\text{m}^2$, providing $\gamma = 7 \times 10^{-4} \text{ W}^{-1} \cdot \text{m}^{-1}$. Our 1.7-nm spectral width would produce a transform-limited hyperbolic secant pulse with a $T_0 = 2.4/1.763\text{-ps}$ pulse-width. For these parameters, the peak pulse power of a soliton formed in this cavity would be 90 W, with a 1.1-mW average power at a 5-MHz repetition rate.

Our average output power at 5-MHz is $\sim 2 \text{ mW}$, providing an average intracavity power of $\sim 10 \text{ mW}$ ($P_{\text{out}}/20\%$). While this number is somewhat higher than our calculated value, it is reasonable due to the high cavity losses and the uncertainty of the gain fiber parameters. In addition, when there are multiple pulses within the cavity the output power increases by $\sim 0.5 \text{ mW}$ per pulse, which is closer to the 1.1-mW average power calculated for the intracavity soliton.

4 Conclusion

Mode-locked optical pulses were produced by using graphene as a saturable absorber in a 1984-nm Tm-based fiber laser. The linear geometry fiber laser achieved lasing at a wavelength $> 150 \text{ nm}$ from the ASE peak by using a FBG at 1984 nm. The 2- μm wavelength fiber technology is improving, but it is not as refined as that of 1550-nm telecommunication technology. Even with these limitations, we were able to overcome the cavity losses and form mode-locked pulse trains at 5- to 20-MHz repetition rates with output powers from 2 to 8 mW. The mode-locked fiber laser operated in the anomalous dispersion regime, without dispersion compensation, and soliton-like operation was observed. Our graphene transfer process enables bonding graphene to any substrate, and in this case bonding to an Ag mirror produced a wavelength-independent SAM, unlike SESAMs which are engineered for specific wavelengths. In addition, due to material issues SESAMs are difficult to engineer at wavelengths longer than 2 μm ; thus, graphene may play a future role as a SAM for creating mode-locked lasers in the mid-IR region. This laser demonstrates the potential for portable mode-locked laser sources in the mid-IR.

Acknowledgments

The authors thank Rafael Gattass and Catalin Florea for useful discussions and borrowed equipment, and Jerry Chappell of Teracomm for use of the AQ 6375. This work was supported by the Office of Naval Research. Luke O. Nyakiti gratefully acknowledges support from the ASEE for post-doctoral fellowship support.

References

1. R. R. Nair et al., "Fine structure constant defines visual transparency of graphene," *Science* **320**(5881), 1308 (2008).
2. Q. Bao et al., "Atomic-layer graphene as a saturable absorber for ultrafast pulsed lasers," *Adv. Funct. Mater.* **19**(19), 3077–3083 (2009).
3. G. Q. Xie et al., "Graphene saturable absorber for Q-switching and mode locking at 2 μm wavelength," *Opt. Mater. Express* **2**(6), 878–883 (2012).
4. D. Popa et al., "Sub 200 fs pulse generation from a graphene mode-locked fiber laser," *Appl. Phys. Lett.* **97**(20), 203106 (2010).
5. Y. Meng et al., "Multiple-soliton dynamic patterns in a graphene mode-locked fiber laser," *Opt. Express* **20**(6), 6685–6692 (2012).
6. P. L. Huang et al., "Stable mode-locked fiber laser based on CVD fabricated graphene saturable absorber," *Opt. Express* **20**(3), 2460–2465 (2012).
7. A. Martinez and S. Yamashita, "10 GHz fundamental mode fiber laser using a graphene saturable absorber," *Appl. Phys. Lett.* **101**(4), 041118 (2012).
8. J.-L. Xu et al., "Graphene saturable absorber mirror for ultra-fast-pulse solid-state laser," *Opt. Lett.* **36**(10), 1948–1950 (2011).
9. G. Xing et al., "The physics of ultrafast saturable absorption in graphene," *Opt. Express* **18**(5), 4564–4573 (2010).
10. J. Ma et al., "Graphene mode-locked femtosecond laser at 2 μm wavelength," *Opt. Lett.* **37**(11), 2085–2087 (2012).
11. J. Liu, Q. Wang, and P. Wang, "High average power picosecond pulse generation from a thulium-doped all-fiber MOPA system," *Opt. Express* **20**(20), 22442–22447 (2012).
12. M. Zhang et al., "Tm-doped fiber laser mode-locked by graphene-polymer composite," *Opt. Express* **20**(22), 25077–25084 (2012).
13. R. C. Sharp et al., "190-fs passively mode-locked thulium fiber laser with a low threshold," *Opt. Lett.* **21**(12), 881–883 (1996).
14. S. Kivistö et al., "Tunable Raman soliton source using mode-locked Tm-Ho fiber laser," *IEEE Photon. Technol. Lett.* **19**(12), 934–936 (2007).
15. C. R. Pollock et al., "Mode locked, and Q-switched Cr:ZnSe laser using a semiconductor saturable absorbing mirror (SESAM)," in *OSA Trends Opt. Photon. Ser.*, C. Denman and I. Sorokina, Eds., Vol. 98, pp. 252–256, Advanced Solid-State Photonics (ASSP), Vienna, Austria (2005).
16. I. T. Sorokina, E. Sorokin, and T. J. Carrig, "Femtosecond pulse generation from a sesam mode-locked Cr:ZnSe laser," in *Conf. Lasers and Electro-Optics and 2006 Quantum Electronics and Laser Science Conference, CLEO/QELS 2006* (2006).
17. B. Bernhardt et al., "Mid-infrared dual-comb spectroscopy with 2.4 μm Cr²⁺:ZnSe femtosecond lasers," *Appl. Phys. B Lasers Opt.* **100**(1), 3–8 (2010).
18. M. Currie et al., "Quantifying pulsed laser induced damage to graphene," *Appl. Phys. Lett.* **99**(21), 211909 (2011).
19. Q. Wang et al., "Graphene on SiC as a Q-switcher for a 2 μm laser," *Opt. Lett.* **37**(3), 395–397 (2012).
20. M. Jiang et al., "Graphene-based passively Q-switched diode-side-pumped Nd:YAG solid laser," *Opt. Commun.* **284**(22), 5353–5356 (2011).
21. J. Liu et al., "Stable nanosecond pulse generation from a graphene-based passively Q-switched Yb-doped fiber laser," *Opt. Lett.* **36**(20), 4008–4010 (2011).
22. B. V. Cunnning, C. L. Brown, and D. Kieplinski, "Low-loss flake-graphene saturable absorber mirror for laser mode-locking at sub-200-fs pulse duration," *Appl. Phys. Lett.* **99**(26), 261109 (2011).
23. X.-L. Li et al., "Large energy laser pulses with high repetition rate by graphene Q-switched solid-state laser," *Opt. Express* **19**(10), 9950–9955 (2011).
24. H. Shen et al., "Passively Q-switched Nd:KLu(WO₄)₂ laser at 1355 nm with graphene on SiC as saturable absorber," *Appl. Phys. Express* **5**(9), 092703 (2012).
25. C. Gao et al., "Resonantly pumped 1.645 μm high repetition rate Er:YAG laser Q-switched by a graphene as a saturable absorber," *Opt. Lett.* **37**(4), 632–634 (2012).
26. E. Sorokin et al., "Sensitive multiplex spectroscopy in the molecular fingerprint 2.4 μm region with a Cr²⁺:ZnSe femtosecond laser," *Opt. Express* **15**(25), 16540–16545 (2007).
27. C. Berger et al., "Ultrathin epitaxial graphite: 2D electron gas properties and a route toward graphene-based nanoelectronics," *J. Phys. Chem.* **108**(52), 19912–19916 (2004).

28. B. L. VanMil et al., "Graphene formation on SiC substrates," *Mater. Sci. Forum* **615–617**, 211–214 (2009).
29. C.-C. Lee, J. M. Miller, and T. R. Schibli, "Doping-induced changes in the saturable absorption of monolayer graphene," *Appl. Phys. B Lasers Opt.* **108**(1), 129–135 (2012).
30. J. D. Caldwell et al., "Technique for the dry transfer of epitaxial graphene onto arbitrary substrates," *ACS Nano* **4**(2), 1108–1114 (2010).
31. Q. Wang et al., "Mode-locked Tm-Ho-codoped fiber laser at 2.06 μm ," *IEEE Photon. Technol. Lett.* **23**(11), 682–684 (2011).
32. S. M. J. Kelly, "Characteristic sideband instability of periodically amplified average soliton," *Electron. Lett.* **28**(8), 806–807 (1992).
33. M. L. Dennis and I. N. Duling III, "Experimental study of sideband generation in femtosecond fiber lasers," *IEEE J. Quant. Electron.* **30**(6), 1469–1477 (1994).
34. J. Geng et al., "Kilowatt-peak-power, single-frequency, pulsed fiber laser near 2 μm ," *Opt. Lett.* **36**(12), 2293–2295 (2011).
35. G. P. Agrawal, *Nonlinear Fiber Optics*, 3rd ed., Academic Press, San Diego (2001).

Biographies and photographs of the authors are not available.